Original Article

# Factors influencing magnetic resonance imaging changes associated with pelvic bone injury after high-intensity focused ultrasound ablation of uterine fibroids: a retrospective case-control study

**Yuhang Liu[1], Furong Lv[1], Yang Liu[1], Yuqing Zhong[2], Ying Qin[1], Fajin Lv[1], Zhibo Xiao[1]**

[1]Department of Radiology, The First Affiliated Hospital of Chongqing Medical University, Chongqing, China; [2]State Key Laboratory of Ultrasound in Medicine and Engineering, College of Biomedical Engineering, Chongqing Medical University, Chongqing, China

*Contributions:* (I) Conception and design: Yuhang Liu, Z Xiao; (II) Administrative support: Furong Lv, Fajin Lv; (III) Provision of study materials or patients: Fajin Lv, Yang Liu; (IV) Collection and assembly of data: Yuhang Liu, Y Zhong, Y Qin; (V) Data analysis and interpretation: Yuhang Liu; (VI) Manuscript writing: All authors; (VII) Final approval of manuscript: All authors.

*Correspondence to:* Zhibo Xiao, PhD. Department of Radiology, The First Affiliated Hospital of Chongqing Medical University, No. 1 Youyi Road, Yuzhong District, Chongqing 400016, China. Email: 202530@cqmu.edu.cn.

**Background:** The application of high-intensity focused ultrasound (HIFU) in the treatment of uterine fibroids is becoming increasingly widespread, and postoperative collateral thermal damage to adjacent tissue has become a prominent subject of discussion. However, there is limited research related to bone injury. Therefore, the aim of this study was to investigate the potential factors influencing unintentional pelvic bone injury after HIFU ablation of uterine fibroids with magnetic resonance imaging (MRI).

**Methods:** A total of 635 patients with fibroids treated with HIFU in the First Affiliated Hospital of Chongqing Medical University were enrolled. All patients underwent contrast-enhanced MRI (CE-MRI) pre- and post-HIFU. Based on the post-treatment MRI, the patients were divided into two groups: pelvic bone injury group and non-injury group, while the specific site of pelvic bone injury of each patient was recorded. The univariate and multivariate analyses were used to assess the correlations between the factors of fibroid features and treatment parameters and pelvic bone injury, and to further analyze the factors influencing the site of injury.

**Results:** Signal changes in the pelvis were observed on CE-MRI in 51% (324/635) of patients after HIFU. Among them, 269 (42.4%) patients developed sacral injuries and 135 (21.3%) had pubic bone injuries. Multivariate analyses showed that patients with higher age [P=0.003; odds ratio (OR), 1.692; 95% confidence interval (CI): 1.191–2.404], large anterior side-to-skin distance of fibroid (P<0.001; OR, 2.297; 95% CI: 1.567–3.365), posterior wall fibroid (P=0.006; OR, 1.897; 95% CI: 1.204–2.989), hyperintensity on T2-weighted imaging (T2WI, P=0.003; OR, 2.125; 95% CI: 1.283–3.518), and large therapeutic dose (TD, P<0.001; OR, 3.007; 95% CI: 2.093–4.319) were at higher risk of postoperative pelvic bone injury. Further analysis of the factors influencing the site of the pelvic bone injury showed that some of the fibroid features and treatment parameters were associated with it. Moreover, some postoperative pain-related adverse events were associated with the pelvic bone injury.

**Conclusions:** Post-HIFU treatment, patients may experience pelvic injuries to the sacrum, pubis, or a combination of both, and some of them experienced adverse events. Some fibroid features and treatment parameters are associated with the injury. Taking its influencing factors into full consideration preoperatively, slowing down treatment, and prolonging intraoperative cooling phase can help optimize treatment decisions for HIFU.

**Keywords:** High-intensity focused ultrasound (HIFU); uterine fibroids; pelvic bone injury; magnetic resonance imaging (MRI); safety

Submitted Mar 14, 2023. Accepted for publication Oct 18, 2023. Published online Jan 02, 2024.
doi: 10.21037/qims-23-323
**View this article at:** https://dx.doi.org/10.21037/qims-23-323

## Introduction

High-intensity focused ultrasound (HIFU) has been shown to be safe and effective for the treatment of uterine fibroids in many studies (1-3). HIFU concentrates ultrasonic beams on target tissues *in vivo* in a certain way, inducing thermal and cavitation effects that can cause irreversible coagulative necrosis and tissue damage (4). Given the physical properties of ultrasound, this thermal ablation therapy may cause collateral thermal damage to adjacent tissue structures in the acoustic field.

Magnetic resonance imaging (MRI) is widely used for the postoperative follow-up of HIFU ablation because of its excellent soft tissue resolution that can assess the target and surrounding tissue. Several studies have investigated postoperative soft tissue damage in non-target areas within the acoustic channel (5-8). However, only a few published studies have evaluated the use of MRI to assess possible bone damage in the pelvis after HIFU and have mostly focused on exploring the sacrococcygeal region located in the posterior acoustic field without specifically investigating other parts of the pelvis (9-12). Nevertheless, such studies are certainly necessary because the pelvis is an important support structure for the human body and an essential component of the parturient canal (13). A large number of women with fibroids who desire fertility could benefit from this noninvasive procedure. During ablation, attention should be paid to the safety of the bone birth canal, which consists of the sacrum, coccyx, and right/left hip bones and their ligaments (14).

In principle, physicians will assess the location of the lesion preoperatively and control the beam path intraoperatively to actively avoid the pubic bone. Since the pubis is located near the anterior acoustic field, the energy transmission of the ultrasonic beam may be obstructed. However, ultrasound can reflect, refract, and scatter within the pelvis, which may create small ectopic foci in non-target tissue where ultrasound energy accumulates and is absorbed, producing unexpected effects (15). Currently, only a limited number of studies have investigated whether the pubic bone located in the anterior pelvic wall and the iliac and sciatic bones on either side are affected by ultrasound energy (12), and no study has specifically evaluated the overall pelvic bone condition after HIFU for uterine fibroids.

Therefore, the aim of this study was to assess the potential MRI signal changes in the pelvic bone after HIFU ablation of uterine fibroids and to further analyze its relationship with fibroid features and treatment parameters to clarify the factors contributing to its vulnerability. We present this article in accordance with the STROBE reporting checklist (available at https://qims.amegroups.com/article/view/10.21037/qims-23-323/rc).

## Methods

### *Patients*

The study was conducted in accordance with the Declaration of Helsinki (as revised in 2013). The study was approved by the Institutional Review Board of the First Affiliated Hospital of Chongqing Medical University in Chongqing, China (approval No. 2021-548), and the requirement for informed consent was waived due to the retrospective nature of the study.

This study was a single-center, retrospective case-control study that reviewed all 1,141 patients who underwent HIFU ablation for uterine fibroids at our hospital between December 2019 and April 2021. The inclusion criteria were as follows: (I) women over the age of 18 with (II) a confirmed clinical diagnosis of uterine fibroids requiring treatment and (III) the ability to communicate with the operator during ablation treatment. The exclusion criteria were: (I) endometriosis or other serious gynecological diseases; (II) previous treatment of uterine fibroids or pelvic disease by HIFU; (III) incomplete preoperative or postoperative pelvic MRI or clinical data; and (IV) pregnancy.

### *MRI evaluation*

MRI examinations (scan parameters are shown in *Table 1*) were performed for each patient before and

 

**Table 1** United imaging MRI acquisition parameters

| Sequence | Repetition time (ms) | Echo time (ms) | Flip angel (°) | Slice thickness (mm) | Slice gap (mm) | Field of view (mm) | Matrix size | Acquisition duration | Imaging plan |
|---|---|---|---|---|---|---|---|---|---|
| T1-FSE | 170.00 | 8.18 | 90 | 5.0 | 2 | 252×360 | 320×224 | 2 min 28 s | Axial |
| T2-FSE-fat suppressed | 4,729.00 | 75.06 | 90 | 5.0 | 2 | 240×240 | 320×240 | 2 min 55 s | Sagittal |
| *T1-weighted quick3D-fat suppressed | 3.97 | 1.84 | 10 | 5.0 | – | 350×280 | 288×216 | 18 s | Sagittal |

*, Scanning with gradient echo sequence. Gd-DTPA (0.1 mmol/kg; Magnevist, Bayer Pharma AG, Germany) was used for contrast enhancement. MRI, magnetic resonance imaging; FSE, fast spin echo.

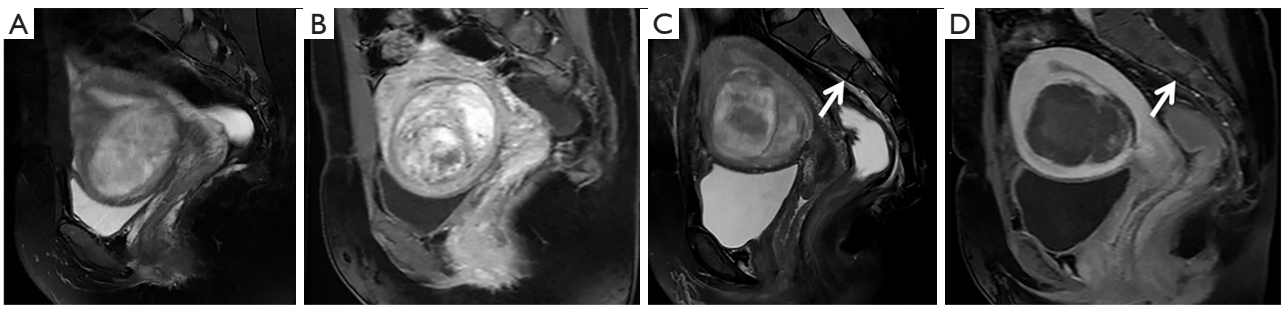


**Figure 1** Patient No. 249, 38 years old. (A,B) MRI images before HIFU ablation; (C,D) MRI images after HIFU. Fat-suppressed T2WI on sagittal image showed a T2-hyperintense (A) and almost significantly enhanced fibroid located in the anterior wall (B); (C) post-HIFU fat-suppressed T2WI image showed a sheet-like hypointense area in the vertebrae of sacral 2 and 3 (arrow); (D) post-HIFU contrast-enhanced image showed an area without enhancement in the vertebrae of sacral 2 and 3 (arrow). MRI, magnetic resonance imaging; HIFU, high intensity focused ultrasound; T2WI, T2-weighted imaging.

1–2 d after HIFU. A magnetic resonance (MR) scanner with 12-channel abdominal coil (1.5-Tesla, uMR570, United Imaging Medical Ltd., Shanghai, China) was used. MR images were evaluated independently by two experienced radiologists (10 and 8 years of experience), blinded to the outcome and patient information before assessment. In case of disagreement, the final decision was made by the chief doctor (20 years of experience) of the department.

Upon comparing pre/post-HIFU MRI images, pelvic bone injuries [T2-weighted imaging (T2WI) images showing an area of sheet-like signal changes, and contrast-enhanced MRI (CE-MRI) revealing a non-enhanced region] were assessed, and the site of injury was recorded (*Figures 1-3*). According to the postoperative MR findings, all of the patients were divided into the following two groups: (I) with pelvic injury and (II) without pelvic injury.

Based on MR images, the following data were collected: fat-suppressed T2-weighted sequence was used to evaluate the distance from the anterior/posterior side of the fibroid to the skin/sacrum, thickness of the abdominal wall, maximal diameter, location of fibroids (anterior, posterior, lateral, fundus), position of the uterus (anteverted, retroverted, mid position), type of fibroids (submucosal, intramural, subserosal), signal intensity of T2WI [hypointense (signal intensity is lower than that of the skeletal muscle or similar), isointense (signal intensity higher than that of the skeletal muscle but lower than the myometrium), hyperintense (signal intensity similar to or higher than that of the myometrium)]; and degree of fibroid enhancement [slight (signal intensity less than that of the myometrium), moderate (signal intensity similar to that of the myometrium), significant (signal intensity higher than that of the myometrium)] was evaluated in enhancement sequence (16). The three-dimensional diameters of the non-perfused area and leiomyoma were measured on CE-MRI images: longitudinal (a), anterior-posterior (b), and transverse (c). Non-perfused volume (NPV) and fibroid volume were calculated based on the following equation: $V=0.5233\times a\times b\times c$, and the NPV ratio (NPV to fibroid volume) was calculated.

 

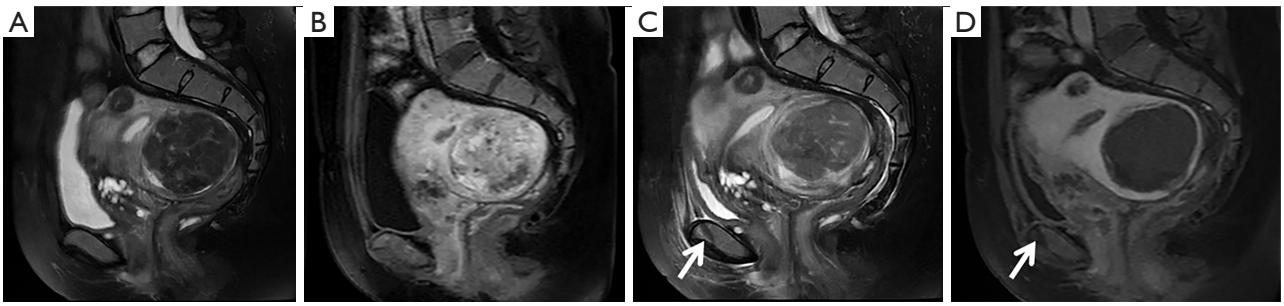


**Figure 2** Patient No. 324, 39 years old. (A,B) MRI images before HIFU ablation; (C,D) MRI images after HIFU. Fat-suppressed T2WI on sagittal image showed a T2-hypointense (A) and moderately enhanced fibroid located in the posterior wall (B); (C) post-HIFU fat-suppressed T2WI image showed a hyperintense center area with hypointense margin in the pubic bone (arrow); (D) post-HIFU contrast-enhanced image showed no enhanced area in the pubic bone (arrow). MRI, magnetic resonance imaging; HIFU, high intensity focused ultrasound; T2WI, T2-weighted imaging.

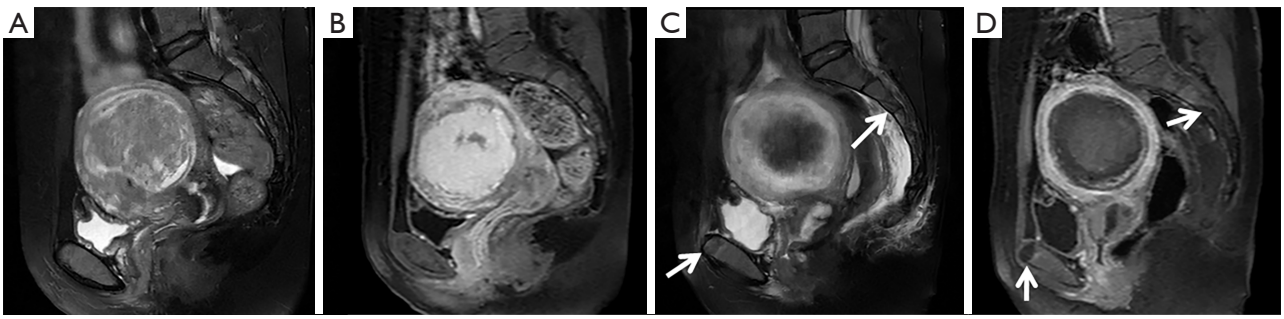


**Figure 3** Patient No. 58, 39 years old. (A,B) MRI images before HIFU ablation; (C,D) MRI images after HIFU. Fat-suppressed T2WI on sagittal image showed a T2-hyperintense (A) and significantly enhanced fibroid located in the anterior wall (B); (C) post-HIFU fat-suppressed T2WI image showed some sheet-like hypointense areas in the pubic bone and vertebrae of sacral 2–4 (arrow); (D) post-HIFU contrast-enhanced image showed no enhanced areas that correspond to the hypointense areas in the pubic bone and vertebrae of sacral 2–4 (arrow). MRI, magnetic resonance imaging; HIFU, high intensity focused ultrasound; T2WI, T2-weighted imaging.

### *HIFU ablation*

All HIFU procedures were performed using a clinical extracorporeal JC200 HIFU therapy system (Chongqing Haifu Medical Technology Co. Ltd., Chongqing, China). A mono-element ultrasound transducer with a frequency of 0.8 MHz, a focal length of 15 cm, and a diameter of 20 cm produced the therapeutic ultrasound beam; the dimensions of the focal region were 3 mm × 3 mm × 8 mm. A Mylab 70 ultrasound imaging device (Esaote, Genova, Italy) was assembled in this system for real-time imaging of fibroids and treatment monitoring with curved array probes and scanning modes including B-mode, M-mode, Color Flow Imaging Mode, Pulsed Doppler, etc. The treatment head can be moved freely in six directions under computer control: left-right (X-axis), head-foot (Y-axis), and up-down (Z-axis), with a range of 120, 120, and 180 mm, respectively.

The ablation was performed with the patient in a prone position, and the abdominal wall of the patient was in contact with circulating degassed water in a tank. During treatment, the patient was under intravenous sedation with fentanyl and midazolam hydrochloride and was able to remain awake throughout the procedure to communicate with the physician and report any intraoperative discomfort or pain. Any patient feedback was recorded. The treatment power, continuous ultrasonic sonication (emission) time, and cooling time were adjusted according to patient tolerance, and the ablation results were assessed in real-time based on the increased gray of the target area as revealed

 

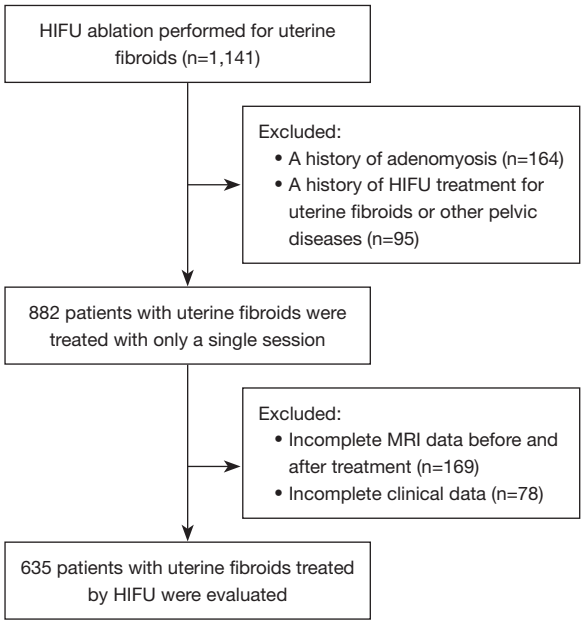


**Figure 4** Flowchart of the inclusion and exclusion decision tree. HIFU, high intensity focused ultrasound; MRI, magnetic resonance imaging.

by B-mode monitoring ultrasound imaging. Treatment was stopped when all signs of blood flow disappeared or grayscale changes in the target tissue were observed on color Doppler ultrasound. The following parameters were recorded: sonication power, sonication time, treatment time, therapeutic dose (TD, KJ, total dose required to ablate the fibroid), treatment intensity (s/h, sonication time required to ablate fibroids per hour), and energy-efficiency factor (EEF, J/mm$^3$, the energy required to ablate per unit volume of fibroids).

Related complications were assessed within one day after ablation by clinicians. We retrieved the relevant data from the clinical information system and recorded it. According to the Society of Interventional Radiology (SIR) classification system, the severity of postoperative adverse events was recorded, including a range of symptoms such as lower abdominal pain, sacrococcygeal pain, vaginal discharge, etc. The classifications were evaluated as follows: (I) class A, no therapy, no consequence; (II) class B, nominal therapy or no consequence, including overnight admission for observation only; (III) class C, therapy and minor hospitalization (<48 h) required; (IV) class D, major therapy required, including an unplanned increase in the level of care or prolonged hospitalization (>48 h); (V) class E, permanent adverse sequelae; and (VI) class F: death (17,18).

### *Statistical analysis*

Normal and skewed distribution measures were expressed as mean ± standard deviation and median with interquartile range, respectively, while count data were expressed as frequencies. The Mann-Whitney test, $\chi^2$ test, and independent sample *t*-test were used to determine the statistical significance of the differences between the groups with or without pelvic bone injury. Pelvic bone injury was set as the dependent variable, whereas fibroid features and clinical parameters were set as independent variables. All variables with P<0.05 in the univariate analysis were selected for binary logistic regression (LR) in the multivariate analysis [stepwise forward (LR) selection] after collinearity diagnostics. The patients were further regrouped according to the site of the pelvic bone injury. A binary LR model with entry and stepwise forward (LR) selection was used for univariate and multivariate analyses of factors associated with the site of pelvic bone injury, respectively. The differences in the incidence of adverse events between the groups with and without pelvic bone injury were compared using the $\chi^2$ test or Fisher's exact test.

Statistical significance was defined as a two-sided P value of <0.05. Data were analyzed using IBM SPSS Statistics software for Windows, version 26.0 (IBM Corp., Armonk, NY, USA).

## Results

### *Baseline characteristics and fibroid features of patients*

The patient inclusion and exclusion criteria are summarized in *Figure 4*. The median age of 635 patients was 42 years (range, 18–56 years). The mean fibroid maximal diameter and volume were 6.48±2.02 cm and 133.28±143.20 cm$^3$, respectively. The mean values of the distance from anterior side of the fibroid to the skin, the distance from posterior side of the fibroid to the sacrum, and the abdominal wall thickness were 48.01±20.77, 27.79±17.59, 26.35±7.59 mm, respectively. Post-HIFU the pelvic bone injury is often observed as poor or no enhancement on CE-MRI. On postoperative MRI, the pelvic bone injury was observed in 324 (51%) patients, while no signal intensity changes were observed in the pelvis of 311 (49%) patients. Of all patients, 269 (42.4%) developed sacral injuries on MR images (*Figure 1*), and 135 (21.3%) experienced pubic bone injuries (*Figure 2*). This included 80 patients who had combined sacral and pubic bone injuries (*Figure 3*). No obvious imaging changes were observed in the iliac or sciatic bones after treatment in any of the 635 patients.

**Table 2** Univariate analysis of the relationship between pelvic bone injury and clinic features

| Characteristics | With injury | Without injury | P value |
|---|---|---|---|
| Samples | 324 (51.0) | 311 (49.0) | |
| Age (years) | 43 [37–46] | 40 [34–45] | 0.001[a] |
| Anterior side of the fibroid to skin (mm) | 48.34 (33.41–65.20) | 39.58 (30.84–53.84) | <0.001[a] |
| Posterior side of the fibroid to sacrum (mm) | 20.33 (13.11–34.53) | 27.52 (14.26–43.11) | <0.001[a] |
| Abdominal wall thickness (mm) | 25.62 (20.97–30.81) | 26.02 (21.08–31.07) | 0.473[a] |
| Fibroid maximal diameter (cm) | 6.21 (5.18–7.46) | 6.23 (5.09–7.45) | 0.547[a] |
| Fibroid volume ($cm^3$) | 91.37 (52.67–167.12) | 85.89 (51.86–168.66) | 0.473[a] |
| Position of uterus | | | 0.004[b] |
| Anteverted | 202 (31.8) | 228 (35.9) | |
| Retroverted | 84 (13.2) | 65 (10.2) | |
| Mid position | 38 (6.0) | 18 (2.8) | |
| Location of fibroids | | | <0.001[b] |
| Anterior wall | 100 (15.7) | 136 (21.4) | |
| Posterior wall | 126 (19.8) | 60 (9.4) | |
| Lateral wall | 82 (12.9) | 86 (13.5) | |
| Fundus | 16 (2.5) | 29 (4.6) | |
| Type of fibroids | | | 0.522[b] |
| Submucosal | 21 (3.3) | 21 (3.3) | |
| Intramural | 260 (40.9) | 239 (37.6) | |
| Subserosal | 43 (6.8) | 51 (8.0) | |
| T2WI | | | <0.001[b] |
| Hypointense | 53 (8.3) | 81 (12.8) | |
| Isointense | 119 (18.7) | 139 (21.9) | |
| Hyperintense | 152 (23.9) | 91 (14.3) | |
| Degree of enhancement | | | <0.001[b] |
| Slight | 108 (17.0) | 143 (22.5) | |
| Moderate | 133 (20.9) | 122 (19.2) | |
| Significant | 83 (13.1) | 46 (7.2) | |

Data are expressed as number (percentage) or median with interquartile range. [a], From the Mann-Whitney U test. [b], From the $\chi^2$ test. T2WI, T2-weighted imaging.

The numbers of patients with uterine fibroids located in the anterior wall, posterior wall, lateral wall, and fundus were 100 (15.7%), 126 (19.8%), 82 (12.9%), and 16 (2.5%) in the pelvic bone injury group, and 136 (21.4%), 60 (9.4%), 86 (13.5%), 29 (4.6%) in the non-injury group, respectively, with significant differences between the two groups. Age (P=0.001), distance from the anterior side of the fibroid to the skin (P<0.001), distance from the posterior side of the fibroid to the sacrum (P<0.001), location of the fibroid (P<0.001), position of the uterus (P=0.004), signal intensity on T2WI of fibroid (P<0.001), and degree of enhancement (P<0.001) were significantly different between the two groups, whereas the differences in thickness of the abdominal wall, maximum diameter of the fibroid, fibroid volume, and type of fibroid were not statistically significant between the two groups (*Table 2*).

**Table 3** Univariate analysis of the relationship between pelvic bone injury and treatment parameters

| Characteristics | With injury (n=324) | Without injury (n=311) | P value |
|---|---|---|---|
| Sonication power (W) | 400 [400–400] | 400 [400–400] | 0.329[a] |
| Treatment intensity (s/h) | 636.75±162.92 | 562.21±151.44 | <0.001[b] |
| TD (KJ) | 480.00 (320.00–715.85) | 312.80 (216.00–460.00) | <0.001[a] |
| EEF (J/mm$^3$) | 4.90 (3.67–6.94) | 3.68 (2.70–5.33) | <0.001[a] |
| NPV (cm$^3$) | 65.13 (36.80–117.33) | 60.26 (34.87–120.56) | 0.482[a] |
| NPV ratio (%) | 0.77 (0.64–0.88) | 0.77 (0.64–0.86) | 0.847[a] |

Data are expressed as mean ± standard deviation or median with interquartile range. [a], From the Mann-Whitney U test. [b], From the independent *t*-test. TD, therapeutic dose; EEF, energy efficiency factor; NPV, non-perfused volume; NPV ratio, ratio (%) of NPV-to-fibroid volume.

| Variables | β | SE | P value | OR [Exp(β)] | 95% CI | | Collinearity statistics | |
|---|---|---|---|---|---|---|---|---|
| | | | | | Lower | Upper | Tolerance | VIF |
| Age (years) | | | | | | | 0.981 | 1.019 |
| ≤40 | | | | | | | | |
| >40 | 0.526 | 0.179 | 0.003 | 1.692 | 1.191 | 2.404 | | |
| Anterior side of the fibroid to skin (mm) | | | | | | | 0.973 | 1.028 |
| ≤48.93 | | | | | | | | |
| >48.93 | 0.832 | 0.195 | <0.001 | 2.297 | 1.567 | 3.365 | | |
| Location of fibroids | | | 0.006 | | | | 0.950 | 1.052 |
| Anterior wall* | | | | | | | | |
| Posterior wall | 0.640 | 0.232 | 0.006 | 1.897 | 1.204 | 2.989 | | |
| Lateral wall | 0.002 | 0.225 | 0.994 | 1.002 | 0.644 | 1.557 | | |
| Fundus | −0.428 | 0.365 | 0.241 | 0.652 | 0.319 | 1.333 | | |
| T2WI | | | 0.003 | | | | 0.839 | 1.192 |
| Hypointense* | | | | | | | | |
| Isointense | 0.150 | 0.238 | 0.528 | 1.162 | 0.729 | 1.853 | | |
| Hyperintense | 0.754 | 0.257 | 0.003 | 2.125 | 1.283 | 3.518 | | |
| TD (KJ) | | | | | | | 0.881 | 1.135 |
| ≤400 | | | | | | | | |
| >400 | 1.101 | 0.185 | <0.001 | 3.007 | 2.093 | 4.319 | | |
| Constant | −1.158 | 0.256 | <0.001 | 0.206 | | | | |

Forest plot

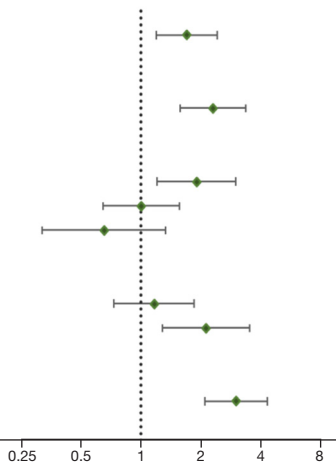


**Figure 5** Binary logistic regression analysis to evaluate factors related to pelvic bone injury. *, Indicates the reference category of contrast in binary logistic regression analysis. With the forward (LR) selection method, the probability for step-wise entry: 0.05, the probability for stepwise removal: 0.10, the classification cutoff: 0.5, and the maximum iterations: 20. β, regression coefficient; SE, standard error; OR, odds ratio; CI, confidence interval; VIF, variance inflation factor; T2WI, T2-weighted imaging; TD, therapeutic dose.

### *Comparison of HIFU treatment parameters between the two groups*

The mean values of sonication power, treatment intensity, TD, EEF, NPV, and NPV ratio for the 635 patients were 392.20±28.76 W, 600.24±161.64 s/h, 450.58±287.81 KJ, 5.23±3.76 J/mm$^3$, 97.96±110.06 cm$^3$, 0.74±0.17, respectively. The median EEF was 4.90 J/mm$^3$ (interquartile range: 3.67–6.94 J/mm$^3$) and 3.68 J/mm$^3$ (interquartile range: 2.70–5.33 J/mm$^3$) in the with and without pelvic bone injury groups, respectively. As shown in *Table 3*, there were significant differences between patients in the pelvic bone injury group and those in the non-injury group in terms of treatment intensity (P<0.001), TD (P<0.001), and EEF (P<0.001). There were no significant differences in sonication power, NPV, and NPV ratio between the two groups (P>0.05).

### *Multivariate analysis of influencing factors of pelvic bone injury*

Variables with significant differences between the two groups in *Tables 2,3* were further included in a multivariate binary LR analysis, as reported in *Figure 5*. In this

 

regression model, the continuous variables were converted to categorical variables based on the cut-off values from the univariate LR. The results showed that age, distance from the anterior side of the fibroid to the skin, fibroid location, T2WI, and TD were independent influencing factors associated with pelvic bone injury (P<0.05).

As shown in *Figure 5*, patients older than 40 years of age were more likely to develop pelvic bone injuries after treatment [P=0.003; odds ratio (OR), 1.692; 95% confidence interval (CI): 1.191–2.404]. When the distance from the anterior side of the fibroid to the skin was greater than 48.93 mm, the risk of pelvic bone injury was higher (P<0.001; OR, 2.297; 95% CI: 1.567–3.365). Patients with fibroids located in the posterior wall had a higher risk of damage to the pelvis after HIFU ablation than those with fibroids located in the anterior wall (P=0.006; OR, 1.897; 95% CI: 1.204–2.989). TD values greater than 400 KJ (P<0.001; OR, 3.007; 95% CI: 2.093–4.319) and higher T2WI signal intensity (P=0.003; OR, 2.125; 95% CI: 1.283–3.518) were associated with a higher probability of pelvic bone injury.

### *Analysis of the factors influencing each site of pelvic bone injury*

Based on the postoperative MR signal intensity changes in the pelvis, we performed further analyses in these patients. Among them, 189 (29.8%) had sacral only injury, 55 (8.7%) had pubic bone only injury, and 80 (12.6%) had injury to both the sacrum and pubic bone (*Table 4*).

With regard to sacral only injury, the following three factors were identified as independent influences by the multivariate model: the distance from the posterior side of the fibroid to the sacrum (P=0.027; OR, 0.988; 95% CI: 0.977–0.999), treatment intensity (P=0.005; OR, 1.002; 95% CI: 1.000–1.003), and EEF (P=0.001; OR, 1.096; 95% CI: 1.040–1.155).

With regard to pubic bone only injury, the following factor was identified as an independent influence by the multivariate analysis: the distance from the anterior side of the myoma to the skin (P<0.001; OR, 1.031; 95% CI: 1.019–1.044, shown in *Table 4*).

Regarding both sacral and pubic bone injuries, we found that age (P<0.001; OR, 1.076; 95% CI: 1.033–1.121), mid-position uterus (P=0.018; OR, 2.469; 95% CI: 1.166–5.225), retroverted uterus (P<0.001; OR, 2.687; 95% CI: 1.546–4.669), and TD (P<0.001; OR, 1.002; 95% CI: 1.001–1.003) were independent risk factors (*Table 4*).

### *Adverse events*

Based on the SIR classification, as shown in *Table 5*, there were 168 (51.9%), 63 (19.4%), 2 (0.6%), and 116 (37.3%), 44 (14.1%), 1 (0.3%) cases of class A, B, and C events in the groups with and without pelvic injury, respectively; no class D, E, or F events occurred in this study. Of all the adverse events that occurred, vaginal discharge had the highest incidence (27.2%; 173/635), with 92 (28.4%) cases in the group with pelvic bone injury and 81 (26.0%) cases in the group without injury. Lower abdominal pain was a relatively common symptom after HIFU, with a significant difference in the incidence of and in the groups with (20.7%; 67/324) and without (13.2%; 41/311) pelvic bone injuries (P=0.012). There were also significant differences in the incidence of sacrococcygeal pain (P=0.004), lower limb numbness/pain (P=0.025), and odynuria (P=0.016) between the two groups. There were no significant differences between the two groups in terms of vaginal discharge, erythema on the skin, nausea and vomiting, proctalgia, or urinary retention (P>0.05).

## Discussion

Despite its clinical significance, to the best of our knowledge, no study has specifically assessed the entire pelvis for bone damage using MRI after HIFU over a patient sample of comparable size. Previously, a few studies investigated the postoperative sacral injury with imaging changes and analyzed the factors influencing them (9-11). Moreover, assessing bone injury with CE-MRI provides an objective image-based endpoint. Compared with the surrounding soft tissue, bones have high acoustic absorption, which can preferentially absorb ultrasonic energy (19). During the ablation of fibroids, the energy deposition caused by the reflection and refraction of ultrasound in the tissue and the direct transfer of energy in the acoustic channel can cause energy to accumulate in the tissue, resulting in ablative heating of the tissue and leading to aseptic inflammation or even necrosis (20,21). The thermal effect of ultrasound can cause fusion of small vessel walls and vascular obliteration, and the cavitation effect can promote energy deposition as well as accelerating blood clotting, destroying the nutrient vessels of the lesion (22-25). Therefore, obstruction of small vessels or vascular compression caused by edema during energy deposition may result in disconnection of the bone-supplying arteries, leading to signal changes in the pelvis on MRI after HIFU,

 

**Table 4** The influencing factors of the site of pelvic injury after HIFU ablation

| Variables | N | Sacrum only (n=189) | | | | Pubis only (n=55) | | | | Sacrum and pubis (n=80) | | | |
|---|---|---|---|---|---|---|---|---|---|---|---|---|---|
| | | Univariable analysis | | Multivariable analysis | | Univariable analysis | | Multivariable analysis | | Univariable analysis | | Multivariable analysis | |
| | | OR (95% CI) | P | OR (95% CI) | P | OR (95% CI) | P | OR (95% CI) | P | OR (95% CI) | P | OR (95% CI) | P |
| Age | 635 | 1.021 (0.995–1.048) | 0.121 | –[¶] | – | 1.000 (0.960–1.042) | 0.993 | –[¶] | – | 1.066 (1.025–1.109) | 0.001 | 1.076 (1.033–1.121) | <0.001 |
| Anterior side of the fibroid to skin | 635 | 0.998 (0.990–1.007) | 0.686 | –[¶] | – | 1.031 (1.019–1.044) | <0.001 | 1.031 (1.019–1.044) | <0.001 | 1.015 (1.005–1.026) | 0.004 | –[¶] | – |
| Posterior side of the fibroid to sacrum | 635 | 0.984 (0.974–0.994) | 0.002 | 0.988 (0.977–0.999) | 0.027 | 0.989 (0.972–1.006) | 0.200 | –[¶] | – | 0.992 (0.978–1.006) | 0.279 | –[¶] | – |
| Abdominal wall thickness | 635 | 0.979 (0.956–1.001) | 0.066 | –[¶] | – | 1.024 (0.989–1.016) | 0.182 | –[¶] | – | 1.004 (0.973–1.035) | 0.816 | –[¶] | – |
| Maximal diameter | 635 | 1.008 (1.000–1.017) | 0.048 | –[¶] | – | 0.986 (0.970–1.002) | 0.078 | –[¶] | – | 0.999 (0.987–1.011) | 0.828 | –[¶] | – |
| Volume | 635 | 1.001 (1.000–1.002) | 0.060 | –[¶] | – | 0.997 (0.994–1.000) | 0.078 | –[¶] | – | 0.999 (0.997–1.001) | 0.375 | –[¶] | – |
| Position of uterus | | | 0.102 | –[¶] | – | | 0.001 | –[¶] | – | | 0.003 | | 0.001 |
| Anteverted* | 430 | | | | | | | | | | | | |
| Retroverted | 149 | 0.639 (0.414–0.986) | 0.043 | | | 2.957 (1.622–5.391) | <0.001 | | | 2.100 (1.240–3.555) | 0.006 | 2.687 (1.546–4.669) | <0.001 |
| Mid position | 56 | 0.934 (0.530–1.645) | 0.728 | | | 2.314 (0.951–5.630) | 0.064 | | | 2.588 (1.266–5.289) | 0.009 | 2.469 (1.166–5.225) | 0.018 |
| Location of fibroids | | | 0.027 | –[¶] | – | | 0.186 | –[¶] | – | | 0.024 | –[¶] | – |
| Anterior wall* | 236 | | | | | | | | | | | | |
| Posterior wall | 186 | 1.852 (1.220–2.812) | 0.004 | | | 1.657 (0.833–3.295) | 0.150 | | | 1.956 (1.124–3.405) | 0.018 | | |
| Lateral wall | 168 | 1.165 (0.745–1.823) | 0.503 | | | 1.650 (0.816–3.338) | 0.164 | | | 0.950 (0.496–1.821) | 0.878 | | |
| Fundus | 45 | 1.091 (0.529–2.249) | 0.814 | | | 0.313 (0.040–2.418) | 0.265 | | | 0.603 (0.174–2.088) | 0.425 | | |
| Type of fibroids | | | 0.465 | –[¶] | – | | 0.895 | –[¶] | – | | 0.422 | –[¶] | – |
| Submucosal* | 42 | | | | | | | | | | | | |
| Intramural | 499 | 0.774 (0.400–1.496) | 0.446 | | | 1.226 (0.364–4.132) | 0.743 | | | 2.016 (0.606–6.709) | 0.253 | | |
| Subserosal | 94 | 0.617 (0.282–1.351) | 0.227 | | | 1.376 (0.353–5.366) | 0.645 | | | 1.548 (0.403–5.940) | 0.525 | | |

**Table 4** *(continued)*

**Table 4** *(continued)*

| Variables | N | Sacrum only (n=189) | | | | Pubis only (n=55) | | | | Sacrum and pubis (n=80) | | | |
|---|---|---|---|---|---|---|---|---|---|---|---|---|---|
| | | Univariable analysis | | Multivariable analysis | | Univariable analysis | | Multivariable analysis | | Univariable analysis | | Multivariable analysis | |
| | | OR (95% CI) | P | OR (95% CI) | P | OR (95% CI) | P | OR (95% CI) | P | OR (95% CI) | P | OR (95% CI) | P |
| T2WI | | | <0.001 | –[¶] | – | | 0.955 | –[¶] | – | | 0.186 | –[¶] | – |
| Hypointense* | 143 | | | | | | | | | | | | |
| Isointense | 258 | 0.442 (0.273–0.714) | 0.001 | | | 0.995 (0.479–2.068) | 0.989 | | | 1.640 (0.801–3.359) | 0.176 | | |
| Hyperintense | 243 | 0.495 (0.337–0.726) | <0.001 | | | 0.912 (0.431–1.928) | 0.809 | | | 1.945 (0.955–3.960) | 0.067 | | |
| Degree of enhancement | | | 0.002 | –[¶] | – | | 0.548 | –[¶] | – | | 0.730 | –[¶] | – |
| Slight* | 251 | | | | | | | | | | | | |
| Moderate | 255 | 1.556 (1.047–2.313) | 0.029 | | | 1.345 (0.711–2.545) | 0.362 | | | 0.848 (0.498–1.444) | 0.543 | | |
| Significant | 129 | 2.298 (1.452–3.638) | <0.001 | | | 1.451 (0.687–3.063) | 0.329 | | | 1.071 (0.577–1.988) | 0.827 | | |
| Sonication power | 635 | 0.997 (0.991–1.003) | 0.334 | –[¶] | – | 1.004 (0.994–1.015) | 0.404 | –[¶] | – | 1.000 (0.992–1.008) | 0.956 | –[¶] | – |
| Treatment intensity | 635 | 1.003 (1.001–1.004) | <0.001 | 1.002 (1.000–1.003) | 0.005 | 1.000 (0.998–1.002) | 0.913 | –[¶] | | 1.002 (1.000–1.003) | 0.026 | –[¶] | – |
| TD | 635 | 1.002 (1.001–1.002) | <0.001 | –[¶] | – | 1.000 (0.999–1.001) | 0.641 | –[¶] | – | 1.002 (1.001–1.002) | <0.001 | 1.002 (1.001–1.003) | <0.001 |
| EEF | 635 | 1.130 (1.074–1.188) | <0.001 | 1.096 (1.040–1.155) | 0.001 | 1.000 (0.930–1.077) | 0.992 | –[¶] | – | 1.042 (0.989–1.098) | 0.124 | –[¶] | – |
| NPV | 635 | 1.002 (1.000–1.003) | 0.043 | –[¶] | – | 0.996 (0.992–1.000) | 0.071 | –[¶] | – | 0.999 (0.997–1.002) | 0.496 | –[¶] | – |
| NPV ratio | 635 | 1.500 (0.558–4.033) | 0.422 | –[¶] | – | 0.262 (0.059–1.171) | 0.080 | –[¶] | – | 1.275 (0.326–4.981) | 0.727 | –[¶] | – |

Univariate analysis was performed with entry method, and all variables with P<0.05 in the univariate analysis were selected for multivariate analysis, which was performed with forward (LR) selection. The probability for step-wise entry: 0.05, the probability for stepwise removal: 0.10, the classification cutoff: 0.5, and the maximum iterations: 20. *, Indicates the reference category of contrast in binary logistic regression analysis. [¶], These items were eliminated in multivariable binary logistic regression analysis with stepwise forward selection. HIFU, high intensity focused ultrasound; OR, odds ratio; CI, confidence interval; T2WI, T2-weighted imaging; TD, therapeutic dose; EEF, energy efficiency factor; NPV, non-perfused volume; NPV ratio, ratio (%) of NPV-to-fibroid volume.

**Table 5** Postoperative adverse events

| Adverse events | With injury (n=324) | | | Without injury (n=311) | | | P value |
|---|---|---|---|---|---|---|---|
| | SIR class A (n=168) | SIR class B (n=63) | SIR class C (n=2) | SIR class A (n=116) | SIR class B (n=44) | SIR class C (n=1) | |
| Vaginal discharge | 92 (28.4) | 0 | 0 | 81 (26.0) | 0 | 0 | 0.506[a] |
| Lower abdominal pain | 38 (11.7) | 29 (9.0) | 0 | 11 (3.5) | 30 (9.6) | 0 | 0.012[a] |
| Sacrococcygeal pain | 19 (5.9) | 14 (4.3) | 0 | 9 (2.9) | 4 (1.3) | 0 | 0.004[a] |
| Lower limb numbness/pain | 5 (1.5) | 12 (3.7) | 0 | 3 (1.0) | 3 (1.0) | 0 | 0.025[a] |
| Erythema on skin | 5 (1.5) | 3 (0.9) | 0 | 2 (0.6) | 1 (0.3) | 0 | 0.146[a] |
| Nausea and vomiting | 6 (1.8) | 5 (1.5) | 0 | 0 | 6 (1.9) | 0 | 0.253[a] |
| Odynuria | 2 (0.6) | 0 | 0 | 10 (3.2) | 0 | 0 | 0.016[a] |
| Proctalgia | 1 (0.3) | 0 | 0 | 0 | 0 | | >0.999[b] |
| Urinary retention | 0 | 0 | 2 (0.6) | 0 | 0 | 1 (0.3) | 0.515[b] |

Data are expressed as n (%). [a], From the $\chi^2$ test; [b], From the fisher's exact test. SIR, the Society of Interventional Radiology.

i.e., demonstrating bone marrow edema on MRI and reduction of osseous perfusion on enhancement sequences (*Figures 1-3*).

Cun *et al.* (9) showed that 39.0% (135/346) of patients with uterine fibroids treated with HIFU developed sacral injuries after ablation. In the present study, 51% (324/635) of the patients showed signal changes on postoperative CE-MRI, i.e., pelvic bone injury. Among these patients, 269 (42.4%) experienced sacral injury and 135 (21.3%) had pubic bone injury, and there were no significant imaging changes in the iliac and sciatic bones. In comparison with the previous study (9), the incidence of sacral injury in this study was similar. The reason for the injuries is that, as a bony structure with a high absorption coefficient perpendicular to or almost perpendicular to the axial acoustic beam energy propagation direction, the energy is easily deposited in the sacrum. Injury of the pubic bone may be caused by its proximity to the anterior acoustic field, the cumulative effect of the anterior field energy during operation, and the reflection and refraction of the acoustic beam resulting in ectopic foci, leading to energy deposition. However, the iliac and sciatic bone in the pelvis had no obvious damage in any of the patients in our study, which may be because they were located below the focal side, far away from the acoustic field, and less affected by ultrasonic energy.

In the present study, patient age, distance from the anterior side of the fibroid to the skin, fibroid location, T2WI, and TD were independent risk factors for pelvic injury (*Figure 5*). As shown in our results, patients older than 40 years of age were more likely to develop pelvic bone injuries after treatment. This is an expected result because the bone mineral density and longitudinal depth of fibroids are predictive of energy absorption and vary from patient to patient. In adulthood, bone density decreases with age (26), leading to decreased scattering of acoustic energy (27), resulting in a more concentrated heating pattern and a consequent possibly increase in the risk of bone damage (19). While the intraoperative delivered ultrasound energy is positively correlated with the depth of focus, deeper lesions are more difficult to ablate (28). In addition, the fibroid location and T2 signal intensity are characteristic parameters that affect the ablation energy of HIFU (28,29). Fan *et al.* (30) showed that fibroids located in the anterior wall or with a low T2 signal were better ablated and required less energy. The TD reflects the energy consumption during HIFU ablation. As a thermal ablation technique, any factor that affects energy deposition in the target area can have an impact on the therapeutic efficiency of HIFU. To reduce the risk of postoperative pelvic injury, patients should be adequately evaluated preoperatively to select suitable patients for treatment; the geometric focus of ultrasound should be as far forward as possible without being too close to sensitive soft tissue structures or the sacrum, pubis, or other bony structures where safety margins discussed in the literature in terms of bony structures include distances ranging from 21 to 30 mm (11,31,32). In addition, to reduce the distance between the

 

fibroid and the transducer, a number of other techniques can be used clinically to achieve the goal, such as filling the rectum with water to push the target fibroid forward, or tilting the beam path to control the heat distribution in the far field.

To further analyze the factors affecting the site of pelvic bone injury, we evaluated the locations of the bone injuries and analyzed the relationship between different injury sites, fibroid features, and treatment parameters (*Table 4*). In the injury group, 189 (29.8%) patients had only sacral injury, 55 (8.7%) had only pubic bone injury, and 80 (12.6%) had both sacral and pubic bone injuries. We found that the smaller the distance from the posterior side of the fibroid to the sacrum, the stronger the treatment intensity, and the greater the EEF, the more inclined the patient was to have a postoperative sacral injury. When the fibroid is close to the sacrum, the focal point of the therapeutic ultrasound beam is also close to the sacrum, which increases the direct conduction of focal domain energy. As the sacrum is supplied by terminal circulation with slower blood flow, the energy is not easily dissipated through the blood flow, and the sacrum is prone to injury (33). The results also indicate that for difficult-to-ablate fibroids with large EEF values, the amount of energy delivered should be controlled intraoperatively to reduce the occurrence of adverse events; simultaneously, the treatment should be slowed down appropriately, and the post-sonication cooling phase should be prolonged to limit the adverse thermal damage caused by cumulative heating. Our study also found that fibroids with greater anterior distances to the skin had a higher risk of post-HIFU pubic bone injury. This phenomenon can be explained by the fact that more energy is required for HIFU of deeply located fibroids (34). In addition, owing to the increased tissue in front of the focal point, the more complex the acoustic interface in the channel is, the higher is the possibility of refractive and reflective interface generation, resulting in unexpected energy deposition and ectopic small focus (35). Moreover, the pubic bone is close to the anterior acoustic field, and although the physician adjusts the therapeutic transducer position during the operation to actively avoid the pubic bone, it cannot be excluded that, in some special cases, the transducer position is lower, and the pubic bone enters the anterior acoustic field to achieve a good ablation effect, thus resulting in energy deposition leading to damage. Therefore, the transducer and focal positions should be appropriately adjusted intraoperatively to avoid pubic bone injury. Meanwhile, we found that the older the patient is, the more posterior is the uterus position, and the greater the TD is, the higher is the likelihood of injury to both the pubic and sacral bones after HIFU. First, the inhomogeneity of both the micro- and macro-structures of soft tissues (e.g., blood vessels, fat pockets, and muscle fibers) may lead to increased scattering of acoustic energy (19,36). The same is true for the bone tissue involved in this study, which has structures such as trabeculae, cortical layers, and a vascular system. The increased scattering results in the dispersion of the heating pattern and a decrease in the heating temperature peak (19). Since increasing age reduces bone density, scattering of the acoustic beam in the bone tissue decreases, favoring less dispersed or more localized energy deposition and possibly making the bone more susceptible to damage. Compared to an anteverted uterus, ablation of a mid or retroverted uterus is more difficult, requiring increased energy and duration of ultrasound irradiation of the intrapelvic tissues (28,37), possibly resulting in thermal damage to both the pubic bone and sacrum. Moreover, the larger the TD is, the greater is the energy in the acoustic field, and the more ultrasonic energy acts on the pelvis, the greater becomes the potential for collateral thermal damage. Łoziński *et al.* (38) demonstrated that pretreatment or periprocedural treatment with vasoconstrictive drugs may reduce heat loss from the peri-ablation circulation and likely improve the efficiency of energy deposition; thus, the reduction in total energy output during ablation may decrease the risk of bone injury.

According to the SIR classification criteria, the incidence of class A, B, and C adverse events occurred in 168 (51.9%), 63 (19.4%), and 2 (0.6%) cases in the pelvic injury group, and 116 (37.3%), 44 (14.1 %), and 1 (0.3%) cases in the non-injury group during the follow-up period, respectively (*Table 5*). No adverse events of class D, E, or F occurred in this study. And the incidence of this study was similar to previous studies (6,10,39). The incidence of postoperative lower abdominal pain, sacrococcygeal pain, and lower limb pain/numbness was higher in the group with pelvic injury than in the group without injury, which was considered to be due to the fact that more energy was required for fibroid ablation in the injury group, and the corresponding soft tissues and nerves were irradiated at an increased dose and at an increased treatment intensity, thus likely causing an increased incidence of corresponding adverse events. All adverse events in this study resolved within one week postoperatively, and enhanced pelvic MRI images can be observed with a gradual decrease in the non-perfused areas of the pelvic bone over a six-month to one-year follow-up

 

period. Therefore, we expect that with increased experience, advances in HIFU technology, and thorough preoperative assessment of patient adaptation conditions, as well as precise control of the focus-tissue interface safety distance, the incidence of adverse events can be further reduced.

The HIFU treatment in our study was ultrasound-guided and performed by a mono-element ultrasound transducer generating a therapeutic beam. Despite its technological maturity and therapeutic efficiency, the inherent characteristics of the device do not allow for real-time temperature monitoring during ablation, as is the case with MRI-guided HIFU therapy. And this was a single-center retrospective study involving multiple analyses of subgroups with potential data selection bias. Therefore, future high-quality, multicenter, prospective studies with large sample sizes are needed to support and verify these conclusions. In addition, patients can be further divided to assess the correlation between whether patients undergo multiple times treatments, and whether they develop postoperative pelvic bone injuries and the degree of injury. Also, we can quantify the area of postoperative pelvic bone injury and conduct a deeper study on the prognosis of bone injury. Moreover, postoperative soft tissue damage combined with pelvic bone injury can also be studied in the future to comprehensively investigate the non-target tissue injury after HIFU treatment for uterine fibroids.

## Conclusions

Some patients developed pelvic bone injuries, including pubic and sacral injuries, after HIFU for uterine fibroids. Patient age, distance from the anterior side of the fibroid to the skin, posterior wall fibroid, T2WI, and TD were independent risk factors for pelvic bone injury. Moreover, some fibroid features and treatment parameters were associated with the injury site. Therefore, to further reduce the incidence of pelvic bone injury, these factors must be fully considered preoperatively, slowing down the treatment speed intraoperatively and focusing on the focus-tissue interface safety distance to optimize the HIFU treatment plan for patients with uterine fibroids.

## Acknowledgments

*Funding:* This study was supported by Chongqing medical scientific research project (Joint project of Chongqing Health Commission and Science and Technology Bureau) (grant number 2021MSXM102).

## Footnote

*Reporting Checklist:* The authors have completed the STROBE reporting checklist. Available at https://qims.amegroups.com/article/view/10.21037/qims-23-323/rc

*Conflicts of Interest:* All authors have completed the ICMJE uniform disclosure form (available at https://qims.amegroups.com/article/view/10.21037/qims-23-323/coif). The authors have no conflicts of interest to declare.

*Ethical Statement:* The authors are accountable for all aspects of the work in ensuring that questions related to the accuracy or integrity of any part of the work are appropriately investigated and resolved. The study was conducted in accordance with the Declaration of Helsinki (as revised in 2013). The study was approved by the Institutional Review Board of the First Affiliated Hospital of Chongqing Medical University in Chongqing, China (approval No. 2021-548), and the requirement for informed consent was waived due to the retrospective nature of the study.



## References

1. Stewart EA, Laughlin-Tommaso SK, Catherino WH, Lalitkumar S, Gupta D, Vollenhoven B. Uterine fibroids. Nat Rev Dis Primers 2016;2:16043.
2. Liu L, Wang T, Lei B. High-intensity focused ultrasound (HIFU) ablation versus surgical interventions for the treatment of symptomatic uterine fibroids: a meta-analysis. Eur Radiol 2022;32:1195-204.
3. Gao H, Li T, Fu D, Wei J. Uterine artery embolization, surgery and high intensity focused ultrasound in the treatment of uterine fibroids: a network meta-analysis. Quant Imaging Med Surg 2021;11:4125-36.
4. Bachu VS, Kedda J, Suk I, Green JJ, Tyler B. High-Intensity Focused Ultrasound: A Review of Mechanisms and Clinical Applications. Ann Biomed Eng

 

2021;49:1975-91.
5. Yin N, Hu L, Xiao ZB, Liu C, Chen WZ, Roberts N, Chen JY, Wang ZB. Factors influencing thermal injury to skin and abdominal wall structures in HIFU ablation of uterine fibroids. Int J Hyperthermia 2018;34:1298-303.
6. Zhang YJ, Xiao ZB, Lv FR, Sheng B, Li J, Zheng YN, Lv FJ, Chen JY. MRI evaluation of endopelvic fascial swelling and analysis of influencing factors in patients with uterine fibroids after high-intensity focused ultrasound ablation. Int J Hyperthermia 2020;37:175-81.
7. Wu CC, Chen WS, Ho MC, Huang KW, Chen CN, Yen JY, Lee PH. Minimizing abdominal wall damage during high-intensity focused ultrasound ablation by inducing artificial ascites. J Acoust Soc Am 2008;124:674-9.
8. Liu Y, Liu Y, Lv F, Zhong Y, Xiao Z, Lv F. Factors influencing magnetic resonance imaging finding of endopelvic fascial edema after ultrasound-guided high-intensity focused ultrasound ablation of uterine fibroids. Int J Hyperthermia 2022;39:1088-96.
9. Cun JP, Fan HJ, Zhao W, Yi GF, Jiang YN, Xie XC. Factors influencing MR changes associated with sacral injury after high-intensity focused ultrasound ablation of uterine fibroids. Int J Hyperthermia 2019;36:21-8.
10. Li D, Gong C, Bai J, Zhang L. Analysis of magnetic resonance signal intensity changes in the sacrococcygeal region of patients with uterine fibroids treated with high intensity focused ultrasound ablation. Int J Hyperthermia 2020;37:404-13.
11. Zheng AQ, Chen JY, Xiao ZB, Zhang R, Bai J. Sacral injury and influencing factors after ultrasonic ablation of uterine fibroids ≤30 mm from the sacrum. Diagn Interv Radiol 2023;29:195-201.
12. Liu Y, Zhang WW, He M, Gong C, Xie B, Wen X, Li D, Zhang L. Adverse effect analysis of high-intensity focused ultrasound in the treatment of benign uterine diseases. Int J Hyperthermia 2018;35:56-61.
13. Stover MD, Edelstein AI, Matta JM. Chronic Anterior Pelvic Instability: Diagnosis and Management. J Am Acad Orthop Surg 2017;25:509-17.
14. Eickmeyer SM. Anatomy and Physiology of the Pelvic Floor. Phys Med Rehabil Clin N Am 2017;28:455-60.
15. Hassanuddin A, Choi JH, Seo DW, Ryu CH, Kim SH, Park DH, Lee SS, Lee SK, Kim MH. Factors affecting tumor ablation during high intensity focused ultrasound treatment. Gut Liver 2014;8:433-7.
16. Chang CT, Jeng CJ, Long CY, Chuang LT, Shen J. High-intensity focused ultrasound treatment for large and small solitary uterine fibroids. Int J Hyperthermia 2022;39:485-9.
17. Lewis CA, Allen TE, Burke DR, Cardella JF, Citron SJ, Cole PE, Drooz AT, Drucker EA, Haskal ZJ, Martin LG, Van Moore A, Neithamer CD, Oglevie SB, Rholl KS, Roberts AC, Sacks D, Sanchez O, Venbrux A, Bakal CW. Quality improvement guidelines for central venous access. The Standards of Practice Committee of the Society of Cardiovascular & Interventional Radiology. J Vasc Interv Radiol 1997;8:475-9.
18. Ahmed M, Solbiati L, Brace CL, Breen DJ, Callstrom MR, Charboneau JW, et al. Image-guided tumor ablation: standardization of terminology and reporting criteria--a 10-year update. Radiology 2014;273:241-60.
19. Hudson TJ, Looi T, Pichardo S, Amaral J, Temple M, Drake JM, Waspe AC. Simulating thermal effects of MR-guided focused ultrasound in cortical bone and its surrounding tissue. Med Phys 2018;45:506-19.
20. Tonguc T, Strunk H, Gonzalez-Carmona MA, Recker F, Lütjohann D, Thudium M, Conrad R, Becher MU, Savchenko O, Davidova D, Luechters G, Mustea A, Strassburg CP, Attenberger U, Pieper CC, Jenne J, Marinova M. US-guided high-intensity focused ultrasound (HIFU) of abdominal tumors: outcome, early ablation-related laboratory changes and inflammatory reaction. A single-center experience from Germany. Int J Hyperthermia 2021;38:65-74.
21. Jenne JW, Preusser T, Günther M. High-intensity focused ultrasound: principles, therapy guidance, simulations and applications. Z Med Phys 2012;22:311-22.
22. Zderic V, Keshavarzi A, Noble ML, Paun M, Sharar SR, Crum LA, Martin RW, Vaezy S. Hemorrhage control in arteries using high-intensity focused ultrasound: a survival study. Ultrasonics 2006;44:46-53.
23. Zhou Y, Ji X, Niu J, Sun T, Qian Z, Li Y, Yuan J, Fan Q, Huang Q, Bai J, Wang Y. Ultrasound-Guided High-Intensity Focused Ultrasound for Devascularization of Uterine Fibroid: A Feasibility Study. Ultrasound Med Biol 2021;47:2622-35.
24. McDannold N, Tempany CM, Fennessy FM, So MJ, Rybicki FJ, Stewart EA, Jolesz FA, Hynynen K. Uterine leiomyomas: MR imaging-based thermometry and thermal dosimetry during focused ultrasound thermal ablation. Radiology 2006;240:263-72.
25. Voogt MJ, van Stralen M, Ikink ME, Deckers R, Vincken KL, Bartels LW, Mali WP, van den Bosch MA. Targeted vessel ablation for more efficient magnetic resonance-guided high-intensity focused ultrasound ablation of uterine fibroids. Cardiovasc Intervent Radiol 2012;35:1205-10.

 

26. Telfer S, Brunnquell CL, Allen JD, Linnau KF, Zamora D, Kleweno CP. The effect of age and sex on pelvic bone density measured opportunistically in clinical CT scans. J Orthop Res 2021;39:485-92.
27. Wear KA. Ultrasonic scattering from cancellous bone: a review. IEEE Trans Ultrason Ferroelectr Freq Control 2008;55:1432-41.
28. Fan HJ, Cun JP, Zhao W, Huang JQ, Yi GF, Yao RH, Gao BL, Li XH. Factors affecting effects of ultrasound guided high intensity focused ultrasound for single uterine fibroids: a retrospective analysis. Int J Hyperthermia 2018;35:534-40.
29. Funaki K, Fukunishi H, Funaki T, Kawakami C. Mid-term outcome of magnetic resonance-guided focused ultrasound surgery for uterine myomas: from six to twelve months after volume reduction. J Minim Invasive Gynecol 2007;14:616-21.
30. Fan HJ, Zhang C, Lei HT, Cun JP, Zhao W, Huang JQ, Zhai Y. Ultrasound-guided high-intensity focused ultrasound in the treatment of uterine fibroids. Medicine (Baltimore) 2019;98:e14566.
31. Yoon SW, Lee C, Cha SH, Yu JS, Na YJ, Kim KA, Jung SG, Kim SJ. Patient selection guidelines in MR-guided focused ultrasound surgery of uterine fibroids: a pictorial guide to relevant findings in screening pelvic MRI. Eur Radiol 2008;18:2997-3006.
32. Pron G. Magnetic Resonance-Guided High-Intensity Focused Ultrasound (MRgHIFU) Treatment of Symptomatic Uterine Fibroids: An Evidence-Based Analysis. Ont Health Technol Assess Ser 2015;15:1-86.
33. Hyvärinen M, Huang Y, David E, Hynynen K. Comparison of computer simulations and clinical treatment results of magnetic resonance-guided focused ultrasound surgery (MRgFUS) of uterine fibroids. Med Phys 2022;49:2101-19.
34. Liu Z, Gong C, Liu Y, Zhang L. Establishment of a scoring system for predicting the difficulty level of high-intensity focussed ultrasound ablation of uterine fibroids. Int J Hyperthermia 2018;34:77-86.
35. deSouza NM, Gedroyc W, Rivens I, Ter Haar G. Tissue specific considerations in implementing high intensity focussed ultrasound under magnetic resonance imaging guidance. Front Oncol 2022;12:1037959.
36. Mahoney K, Fjield T, Mcdannold N, Clement G, Hynynen K. Comparison of modelled and observed in vivo temperature elevations induced by focused ultrasound: implications for treatment planning. Phys Med Biol 2001;46:1785-98.
37. Zhang W, He M, Huang G, He J. A comparison of ultrasound-guided high intensity focused ultrasound for the treatment of uterine fibroids in patients with an anteverted uterus and a retroverted uterus. Int J Hyperthermia 2016;32:623-9.
38. Łoziński T, Ludwin A, Filipowska J, Zgliczyńska M, Węgrzyn P, Kluz T, Ciebiera M. Oxytocin and Misoprostol With Diclofenac in the Preparation for Magnetic Resonance-Guided High-Intensity Ultrasound Treatment of Symptomatic Uterine Fibroids: A Prospective Cohort Study. Ultrasound Med Biol 2021;47:1573-85.
39. Chen J, Chen W, Zhang L, Li K, Peng S, He M, Hu L. Safety of ultrasound-guided ultrasound ablation for uterine fibroids and adenomyosis: A review of 9988 cases. Ultrason Sonochem 2015;27:671-6.

**Cite this article as:** Liu Y, Lv F, Liu Y, Zhong Y, Qin Y, Lv F, Xiao Z. Factors influencing magnetic resonance imaging changes associated with pelvic bone injury after high-intensity focused ultrasound ablation of uterine fibroids: a retrospective case-control study. Quant Imaging Med Surg 2024;14(1):179-193. doi: 10.21037/qims-23-323

 